J Mater Sci (2009) 44:563–571
DOI 10.1007/s10853-008-3071-6

Growth mechanism of ZnO nanowires via direct Zn evaporation

Hao Tang · Jack C. Chang · Yueyue Shan · D. D. D. Ma · Tsz-Yan Lui · Juan A. Zapien · Chun-Sing Lee · Shuit-Tong Lee

Received: 30 March 2008 / Accepted: 20 October 2008 / Published online: 23 November 2008

Abstract Zinc oxide (ZnO) nanowire synthesized from direct Zinc (Zn) vapor transport in O_2 environment has been studied. The results show that the first step is the formation of ZnO film on the substrate. Then anisotropic abnormal grain growth in the form of ZnO platelets takes place. Subsequently, single-crystalline ZnO platelets grow in [0001] direction to form whiskers. During whisker growth, transformation from layer-by-layer growth to simultaneous multilayer growth occurs when the two-dimensional (2D) Ehrlich–Schwoebel (ES) barrier at the ZnO island edge is sufficiently large and the monolayer island diameter is smaller than the island spacing. As multilayered islands grows far away from the base, isotropic mass diffusion (spherical diffusion) will gradually displace anisotropic diffusion (linear diffusion), which contributes to the formation of pyramid on the top plane of the whisker. When the pyramid contains enough atomic layers, the 2D ES barrier transits to 3-dimensional ES barrier, which contributes to repeated nucleation and growth of multilayered islands or pyramids on the old pyramids. The pyramids play a critical role to taper the whisker to nanorod with a diameter less than 100 nm. The nanorod then grows to nanowire via repeated growth of epitaxial hexagonal-pyramid shape-like islands on the (0001)-plane with $\{11\bar{2}3\}$ facets as the slope planes. During coarsening, the breakage of step motion of $\{11\bar{2}3\}$ facets and the appearance of $\{11\bar{2}0\}$ facets on the base of pyramids may result from the step bunching of {0001} facets, which is consistent with the existence of "2D" Ehrlich–Schwoebel barrier on the edge of (0001) facets.

Electronic supplementary material The online version of this article (doi:10.1007/s10853-008-3071-6) contains supplementary material, which is available to authorized users.

H. Tang · J. C. Chang · Y. Shan · D. D. D. Ma · T.-Y. Lui · J. A. Zapien · C.-S. Lee · S.-T. Lee (✉)
Center of Super-Diamond and Advanced Films (COSDAF) & Department of Physics and Materials Science, City University of Hong Kong, Hong Kong SAR, China
e-mail: apannale@cityu.edu.hk

J. C. Chang
Nano-organic Photoelectronic Laboratory, Technical Institute of Physics and Chemistry, Chinese Academy of Sciences, Beijing 100080, China

Introduction

Semiconductor nanowires represent an ideal system for investigating physics and chemistry of low-dimensional materials and are expected to play an important role as building blocks for nano-electronics and nano-photonic devices [1, 2]. It is of both scientific and technological importance to develop a better understanding of the growth mechanisms to realize controlled synthesis of nanowires. Various methods have been suggested for nanowire growth; notably they include (1) Template-induced growth, where carbon nanotubes, zeolites, AAO, or other 1-D volume-controlled structures are used as templates [3]. (2) Vapor–liquid–solid growth, where eutectic alloy or catalyst acts as the energetically favored site for the absorption of gas-phase reactants, and directs and controls the growth [4]. (3) Vapor–solid growth, where diffusion, adsorption, and attachment of reacting atomic species and clusters vaporized from solid are directly deposited to form nanowires [5]. (4) Solution–liquid–solid growth, which is similar to the growth process of vapor–liquid–solid method but takes place in solution [6]. (5) Oxide-assisted growth, where oxidation-reduction reactions plays the dominant

role in the nucleation and growth of high-quality semiconductor nanowires [7].

Recently, a different approach, involving the use of low-melting metal in reactive gas for multiple nucleation and direct growth of nanowires, has been reported. Examples of this include growth of nitrides in ammonia (GaN [8], AlN [9], InN [10]), and oxides in oxygen-containing atmosphere (β-Ga_2O_3 [11], ZnO [12–17], MgO [12, 18], and Nb_2O_5 [19]). The mechanism of InN nanowire growth in reactive vapor transport-NH_3 [10] has been elucidated that nucleation of InN crystals occurs first on the substrate, and then droplet-led growth of the underlying crystals takes place to form one-dimensional nanowires, in a way similar to the VLS mechanism for nanowire growth. However, the growth mechanisms of semiconducting oxide nanowires via direct evaporation of low-melting metal in an O_2-containing environment remain not yet fully understood. Sears' [20] explanation that the whisker growth is induced by axial dislocations and controlled by diffusion of adatoms on the side surface of the whisker to the growth tip is not applicable to the growth of semiconducting oxide nanowires, because the grown wires are nearly free of dislocations.[21] Sharma et al. [11] and Dang et al. [12] suggested a self-catalytic growth mechanism, in which oxygenated metal species dissolved in a molten metal catalyst induces phase segregation and produces multiple nuclei, which grow homoepitaxially into one-dimensional structures from the dissolved species assisted by the high surface tension at the molten metal/metal oxide interface. This direct growth method is highly attractive since it can produce oxide nanowires at high purity (no catalyst contamination), good morphology, fast growth rate (compared to MOCVD method) and energy efficient. A clear understanding of the nanowire growth process is necessary to reveal the growth mechanisms and to realize controllable synthesis. In this article, we study the growth mechanisms of ZnO nanowires via direct Zn evaporation in oxygen atmosphere. In addition, the ZnO nanowires thus synthesized are important because they show strong band gap emission at 3.29 eV, but little defect emission at 2.5 eV [17].

Experimental

The synthesis of ZnO nanowires was carried out in a horizontal three-zone furnace with Ar/O_2 mixture (Ar: 99.995%, 500 sccm; O_2: 99.995%, 5 sccm) as carrier gas, as shown in the schematic in Fig. 1. Zinc powder (200 meshes, 99.995%, Sigma-Aldrich) in a quartz boat was placed in the center of a quartz tube that was inserted into the furnace. Various substrates including single-crystal silicon (Si (100), Si (111)), polycrystalline alumina

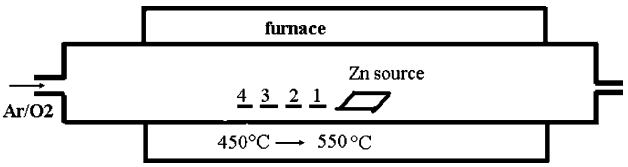

Fig. 1 Experimental setup for ZnO nanowire synthesis via direct Zn evaporation in oxygen

(Al_2O_3), polycrystalline zinc oxide (ZnO), and molybdenum (Mo) were used as the substrates for nanowire growth. The substrates were placed upstream at the boundary of the quartz boat. Zn powders were heated to 550 °C to generate Zn vapor, which oxidized by O_2 and led to the growth of ZnO nanostructures on the substrate at 100 mTorr. Reactor pressure ranging from 50 to 300 mTorr was used in experiments to study the pressure effect on the growth. The substrates were maintained in a temperature range from 450 to 550 °C. The substrates were divided into four parts according to the morphologies of the products deposited on them for ease of analysis. The growth time was typically 60 min and the as-deposited products were characterized using scanning electron microscopy (SEM), transmission electron microscopy (TEM), high-resolution transmission electron microscopy (HRTEM), and X-ray diffraction (XRD).

Results and discussion

To understand the nucleation and growth mechanisms involved in the formation of ZnO nanowires, a short reaction time experiment was performed. The source was heated to 550 °C and kept at this temperature for only 3 min using Si (100) as the substrate. After a 3-min run, the heating process and oxygen supply was stopped with a rapid vacuum pump down. The ZnO product on Si (100) substrate at 500 °C was in the form of a thin ZnO film with bigger ZnO platelets on it (Fig. 2a and b).

Then the reaction time of the experiment was extended to 60 min to study the morphology, phase and growth direction of the product to reveal information regarding the growth mechanism. In the first zone, closest to the ZnO source and at the highest deposition temperature, ZnO whiskers nearly vertically grew out of the ZnO film along the direction of [0001] with some macroscopic steps on their side surfaces (Fig. 3a, b). The large whiskers had diameters in the range of 0.4–0.8 μm, whereas the smaller diameter whiskers showed mound-like morphology with the plate size decreasing from the base to the top. Only (10L) peaks (with L = 0, 1, 2, 3) were observed in the XRD spectra (in supporting information), implying that the ZnO crystals were oriented with some tilting toward the

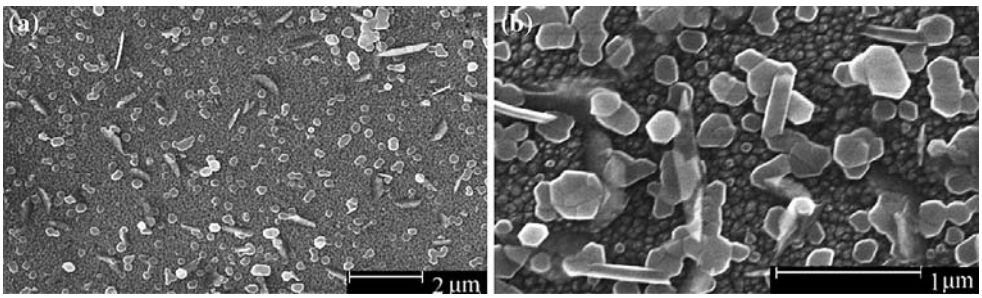

Fig. 2 **a**, **b** SEM images of ZnO samples deposited on silicon after 3-min reaction time

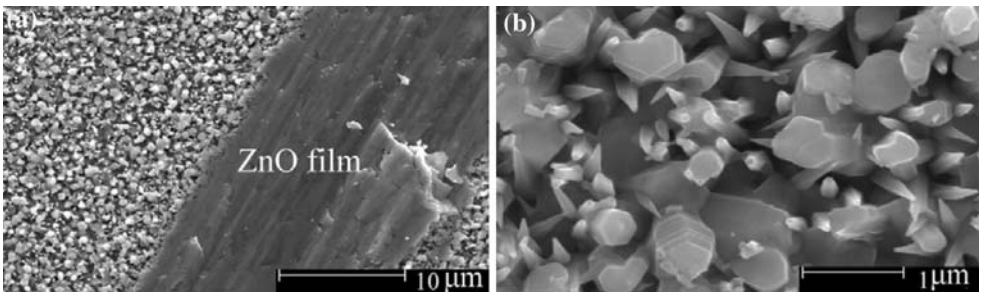

Fig. 3 **a**, **b** SEM images of the sample in the first zone, showing mainly ZnO whiskers on ZnO film deposited on silicon substrate

vertical direction. The intense ZnO diffraction peaks indicate that the products were high-purity ZnO wurtzite phase. The nucleation of ZnO crystals and formation of a film prior to nanowire growth have been reported by others [13]. Similarly, formation of micro-crystalline film before nanowire growth was also observed in InN, GaN, and AlN [8–10] via direct metal evaporation in NH_3.

Figure 4a and b shows that the morphology of ZnO sample deposited in the second zone. The diameter of the whiskers is smaller (about 0.4 μm) compared to that in the first zone (0.4–0.8 μm), and the orientations of the former whiskers were also less uniform. On top of the whisker, the mound grew epitaxially, followed by the growth into pyramid and finally nanorod.

Scanning electron microscopy images of the ZnO sample in the third zone show a nano-pen-like structure, which consists of three parts: a whisker at the bottom, a nanorod at the top, and a pyramidal structure connecting the former two parts, as shown in Fig. 5a–f. The pyramid grows epitaxially on the (0001) plane—the top plane of whisker, and shows some macroscopic steps on the sides. The sidewall faces of the slope on the lower part of the pyramid seem to have hexagonal-symmetry planes. However, this feature is not completely developed due to the slope on the upper part (Fig. 5b and c). The base of the pyramid seems to have rotated by 30° with respect to $\{10\bar{1}0\}$ facets of the host whisker, and the angle between the pyramid sidewall facets and the c-facet is between 45 and 50°, which indicates that the sidewall facets of the pyramid may be $\{11\bar{2}3\}$. The hexagonal prism with six sidewall facets $\{11\bar{2}0\}$ (Fig. 5d and e) or dodecagonal prism bounded by $\{11\bar{2}0\}$ and $\{10\bar{1}0\}$ (Fig. 5f) may also appear on the base of the pyramid from which the nanorod grew. These features may be related to the coarsening effect during nanorod growth. Interestingly, the pyramidal structure including a pyramid on a hexagonal prism can repeatedly grow on the top plane-{0001} facets of the same structure (Fig. 5d and f). On the (0001) top plane of the pyramid, the nanorod grew out with the sidewall facets $\{10\bar{1}0\}$. However, the bottom of the nanorod only occupies the center part of the {0001} top plane; therefore, the {0001} facet terrace at the bottom of the nanorod can be clearly demonstrated in Fig. 5b and d–f.

Transmission electron microscopy images of the typical ZnO nano-pen morphology obtained in the third zone are shown in Fig. 6a–c. The diameters of the nanorods are between 75 and 95 nm; however, those of the host whiskers are about 250 nm. It should be pointed out that when the substrate was farther away from the source, the diameter of the deposited whiskers decreased from 300 to 150 nm gradually due to temperature gradient. The nanorods grown on the whisker have diameters of 65–95 nm and lengths of 100 nm to several microns. The bottom of the whisker is rough as a result of breaking away from the film by its own weight during growth or removal from the substrate by sonification (Fig. 6a). The tip of nanorod is also in the form of a pyramid (Fig. 6c). The angle between the pyramid facets and the c-plane is 47°, which indicates that the pyramid facets are also $\{11\bar{2}3\}$. Electron diffraction patterns of

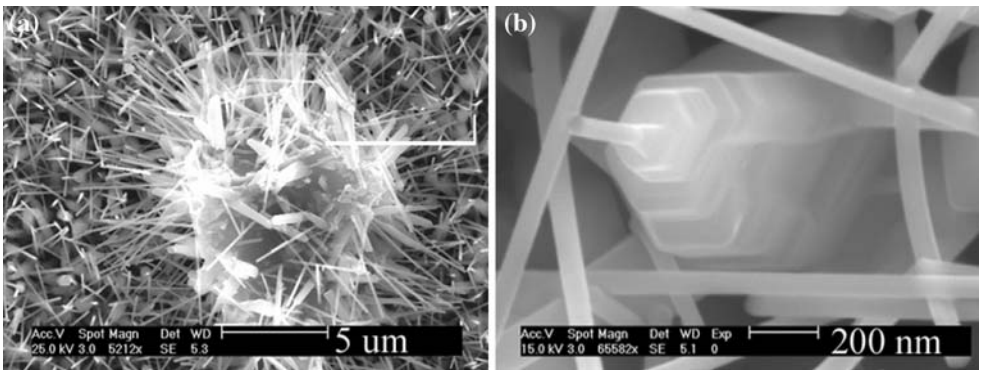

Fig. 4 **a**, **b** SEM images of ZnO sample in the second zone. The nanorod grows on a pyramid, which in turn epitaxially grows on a ZnO whisker. The upper layer of the whisker exhibits mound morphology with decreasing diameter

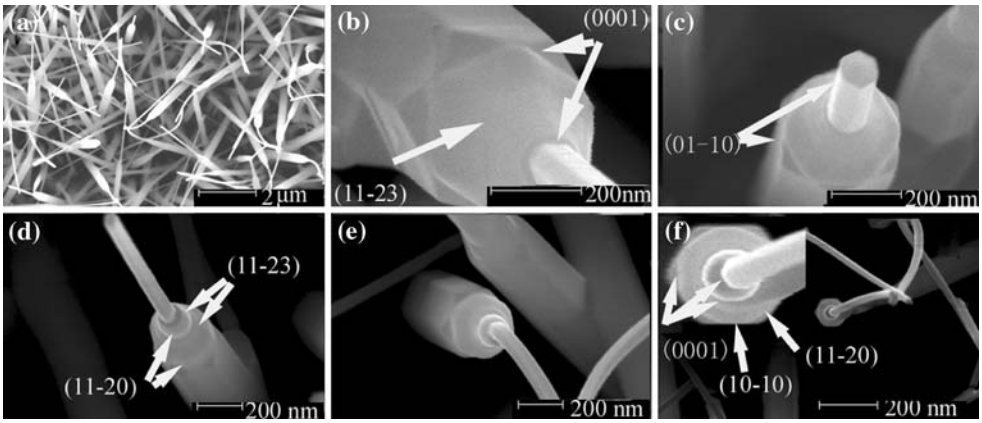

Fig. 5 **a**–**f** SEM images of ZnO sample in the third zone showing a nano-pen-like structure, which consists of three parts: a whisker at the bottom, a nanorod at the tip, and a pyramid connecting the former two parts

the nanorod and pyramid establish that the ZnO samples are single-crystalline wurtzite structure (The electron diffraction of the pyramid shown in Fig. 6d is taken along the $[2\bar{1}\bar{1}0]$ zone axis, and that of the nanorod shown in Fig. 6e is taken along $[01\bar{1}0]$ zone axis). A detailed characterization of the crystalline quality of the sample was carried out by HRTEM (Fig. 6f–h) and the results confirm that whisker, pyramid, and nanorod are perfect crystals without any dislocation. There exist some thick fringes on the sides of the pyramid (Fig. 6g) due to the gradual change of diameter. The pyramid plays a critical role to taper the whisker to nanorod with a diameter less than 100 nm. Afterward, nanorods continued to grow into nanowires, as can be observed in the fourth zone shown in Fig. 7a and b.

Various substrates were used in our experiments, but the growth behaviors did not change. Thus, we conclude that substrates have no or little effect on the growth mechanisms. Changing the reaction pressure or lowering the evaporating temperature (for example to 500 °C) only reduced the wire diameter, but had no other influence on the growth process. The above experimental results provide revealing insight into the growth mechanisms of ZnO nanowires, which is considered to involve four stages as illustrated schematically in Fig. 8.

1. *Nucleation*: Nucleation of ZnO crystals and formation of ZnO film occur first on the substrate (Fig. 8-1).
2. *Platelet Formation*: The large ZnO single crystals in the form of platelets grow on the ZnO film, which is formed by an anisotropic abnormal grain growth process [22] (Fig. 8-2). Such anisotropic growth is due to different surface energies of different crystal planes [23, 24]. The surface energy of polar surface (0001) of ZnO is about 4.3 J/m^2, which is much higher than that of other facets [25], and therefore [0001] becomes the fastest anisotropic abnormal grain growth direction. The platelets continue to grow in the form of whiskers led by the polar surface (0001) of ZnO [26, 27].
3. *Homoepitaxial growth of mound or pyramid on whisker* (Fig. 8-3). During whisker growth, there exists a transformation from layer-to-layer growth to simultaneous multilayer growth, which is responsible for the formation of pyramids. Concurrently, isotropic diffusion will gradually displace anisotropic diffusion. This

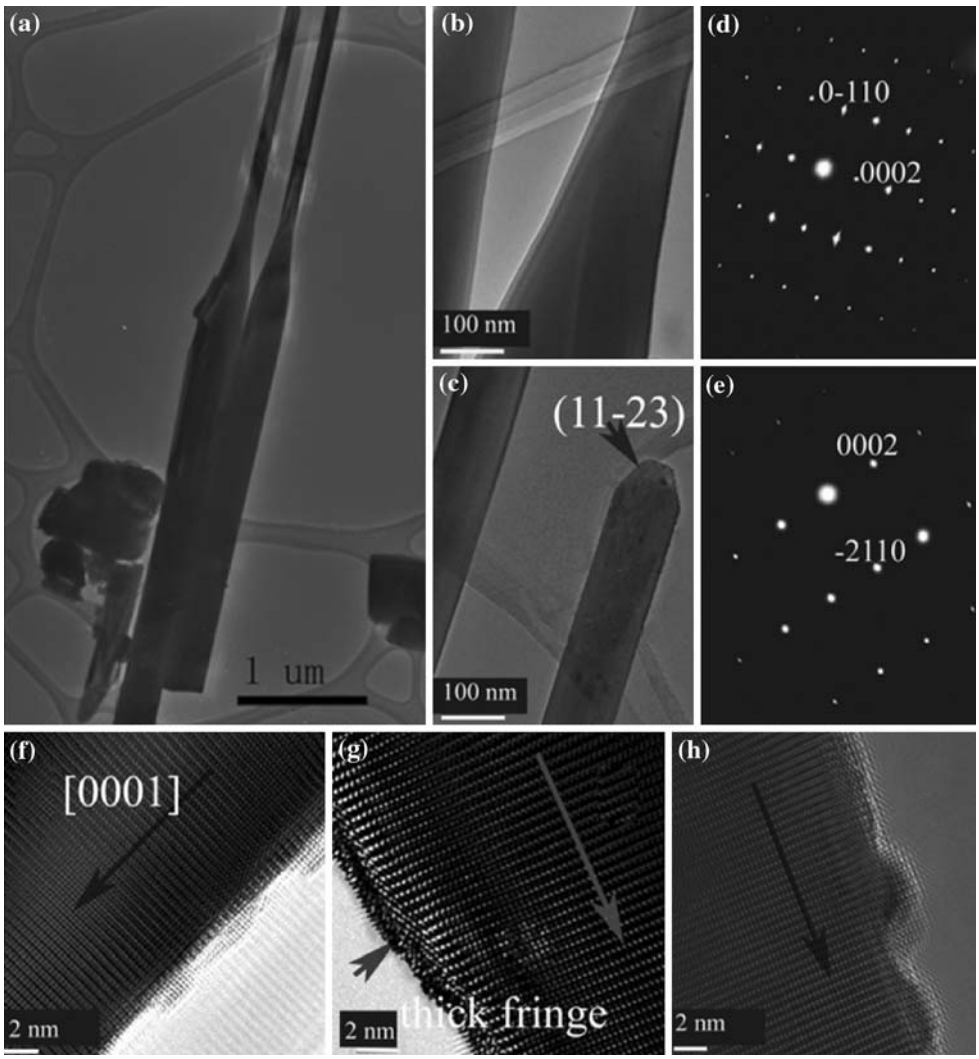

Fig. 6 **a** TEM image of a typical ZnO nanorod on a whisker connected via a pyramid. **b** and **c** TEM images of pyramid and nanorod, respectively. **d** and **e** Corresponding electron diffraction pattern of the pyramid in (**b**) and nanorod in (**c**). **f–h** High-resolution TEM images of the whisker, pyramid, and nanorod, respectively

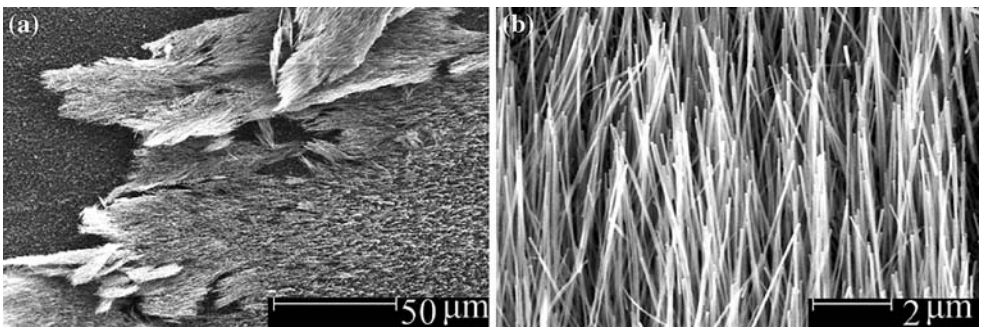

Fig. 7 **a**, **b** SEM images of nanowires deposited in the fourth zone

stage is the key transition point from micro- to nano-structure.

4. *Growth of nanowire on top of pyramid* (Fig. 8-4). In this stage, the nanorod grows to nanowire with a constant diameter.

Stages 3 and 4 are the critical steps responsible for the transformation from micro-structure (whisker or platelet) to nano-structure (nanowire with a diameter less than 100 nm). We will give a more detailed discussion to elucidate the growth mechanism.

The repeated appearance of hexagonal-pyramid shape-like islands bounding by high index facets $\{11\bar{2}3\}$ in the middle and at the end of ZnO nanostructures cannot be explained satisfactorily by any other models, but can be reasonably explained by the Ehrilich–Schwoebel barriers

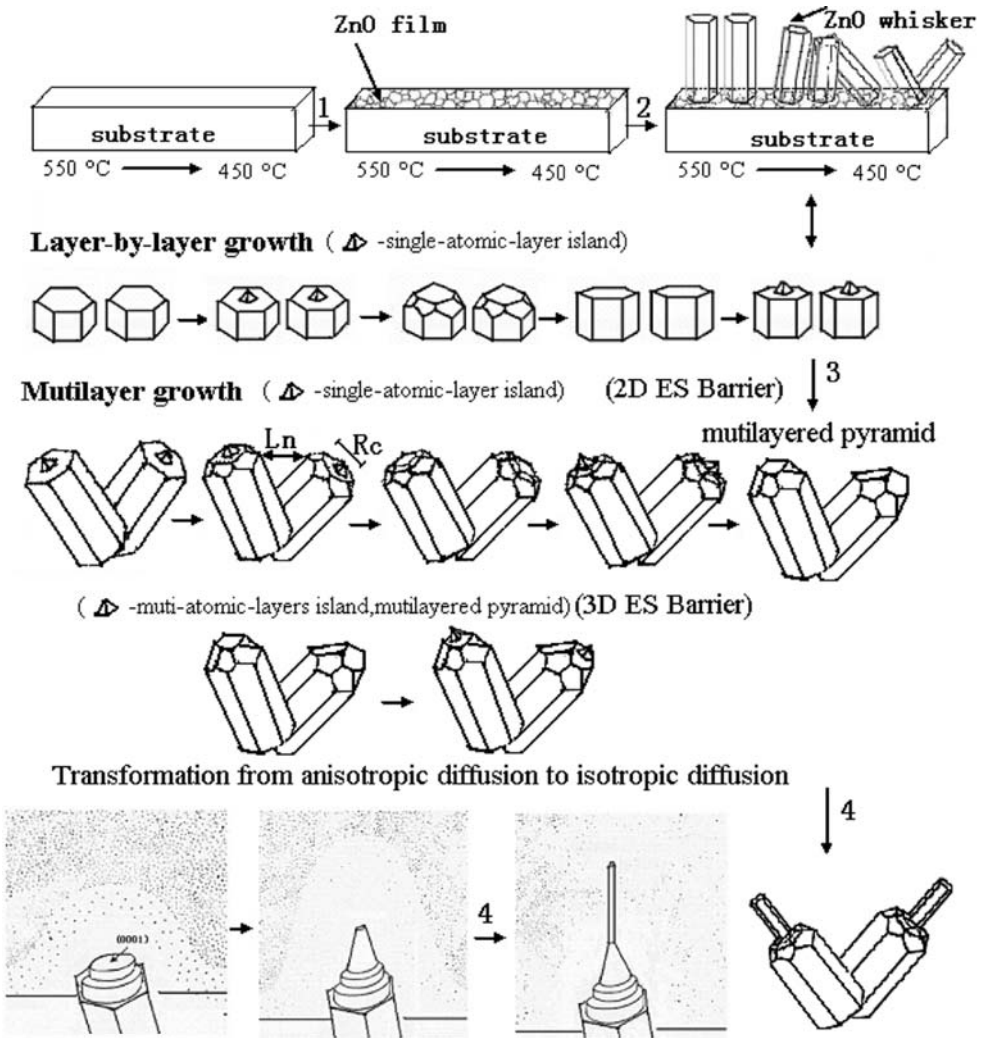

Fig. 8 Schematic of the growth mechanism of ZnO nanowires synthesized via the transport of Zn vapor in the presence of O_2. Stage 1 is the formation of ZnO film. Stage 2 involves anisotropic abnormal growth of single-crystal ZnO in the form of whiskers, followed by layer-by-layer growth. Stage 3, transformation from layer-to-layer to multilayer growth occurs when the Rc < Ln (Rc is the diameter of the base island and Ln the island spacing). When the pyramid composed of multilayered islands grows far away from the base, an isotropic diffusion (spherical diffusion) gradually displaces the anisotropic diffusion (linear diffusion). Once the pyramid involves enough atomic layers to realize transition from 2D ES barrier to 3D ES barrier, a new multilayered island or pyramid would nucleate and grow on the old pyramids. Stage 4, the nanorod grows to nanowire with a constant diameter

(ES barrier) model [28, 29]. The three-dimensional structures such as mound or pyramid on the film are a non-equilibrium effect resulting from microscopic Ehrlich–Schwoebel barriers. The mound or pyramid existing on ZnO whisker is a strong support of the existence of ES barrier on the (0001) ZnO surface, which indicates the existence of an activation barrier at the edge of (0001) plane for interlayer mass transport, hindering the diffusion of ad-species from the upper to the lower levels. The effect of the island-edge barrier (ES barrier) on the film morphology has recently been explored [30–33]. If the ES barrier effect is strong, the important consequence is the destabilization of a singular surface during growth, leading to formation of monolayer islands. Since atoms deposited on top of islands are inhibited from diffusing over the edges, the atoms would remain longer and therefore accumulate easier, resulting in an increased nucleation rate of a new layer. When the mode of growth of multilayer is applied, the formation of a new monolayer islands on top of old islands results in a three-dimensional structure-pyramids or -mounds. On the other hand, if the ES barrier effect is weak, the system can follow layer-by-layer growth and easily reach a stable growth regime with a smooth growth front. The strong regime of the ES barrier effect is separated from the weak regime by Rc = Ln, where Rc is the critical island radius at which a second layer nucleates on the island and Ln is the island spacing [34]. If Rc < Ln, the ES barrier effect is strong enough to cause rough growth; otherwise the effect is weak and the growth mode is smooth. In the case of whisker growth, in the beginning stage the nearly vertical growth of epitaxial ZnO whiskers leads to high density and a film-like morphology, so the ES barrier effect may also govern the growth of ZnO whiskers.

There also exist other processes, such as exchange effects [35], knockout processes [36] and step permeability or transparency [37], which can produce diffusion flux that flows preferentially downhill. These processes can counterbalance the ES barrier effect and, therefore, lead to the selection of one or more slopes at which the net flux in the non-equilibrium situation is equal to zero [32]. The

symmetry of the growth of crystal lattice, of course, has strong effects on the selection of slope: if the side facets of the three-dimensional structure are singular surfaces on which the diffusion current must be zero, then the first such facets encountered is stable. From the images of SEM and TEM, the facets $\{11\bar{2}3\}$ on the epitaxial hexagonal-pyramid shape-like island can be deduced to be the slope that corresponds to the zero surface flux, which is consistent with the observation by Baxter [38].

In the above discussion, the ES effect is only treated as "2D" ES barrier. However, Liu et al. [39] proposed that there was also a "3D" ES barrier, i.e., the additional barrier that must be surmounted by a particle transport from one facet cross the step edge to the adjacent facet. They showed that, for transitions over a step edge between adjacent terraces, the 2D barrier would become a 3D barrier when the height difference between the two terraces increased. There might also be a 3D barrier on $\{11\bar{2}3\}$ facet in the ZnO sample that hindered the diffusion from (0001) facet on the upper layer to (0001) facet to the lower layer, which contributed to the formation of repeated pyramidal structures (as shown in Fig. 5d–f). That is, the atoms deposited on top of the formed multilayered pyramid were inhibited by 3D ES barrier; the atom would remain longer and therefore accumulate easier, resulting in an increased nucleation rate of a new multilayered pyramids or islands on the old ones. Baxter et al. [38] also observed the multilayered islands or pyramids epitaxially grown on the formed multilayered pyramid, but they just used the 2D ES to explain the phenomenon. The detailed mechanisms, such as the number of atomic layers to complete the gradual transition of an ES barrier from 2D to 3D, the magnitude of 3D ES barrier, etc., are however not clear.

It should be emphasized that during multilayer growth, there also exists a mode change of mass diffusion (Fig. 8). As the whiskers begin to grow out of the film to a distance of several tens of nanometers, anisotropic diffusion (linear diffusion) dominates [20, 40]. As the multilayered islands grow and summits rise, the growth no longer depends on anisotropic diffusion of materials. Gradually, it would approach isotropic diffusion (spherical diffusion) [20]. Anisotropic diffusion is known to be important on a number of semiconductor surfaces. Siegert et al. [31] suggested in their model that for the case of anisotropic diffusion and symmetric ES barriers, the steady-state shapes were elongated "mounds", similar to those seen in experiments on GaAs [41]. However, for isotropic diffusion and symmetric ES barriers, the steady-state morphology was symmetric pyramid as was found for Cu(001) [31].

In the first zone, whiskers grow closely and almost all in the same direction, and follow the layer-by-layer growth, showing no obvious change of diameter from the base to the top (Fig. 3b). In the second zone, the substrate is at a lower temperature, whiskers tend to grow more randomly in direction and with smaller diameters, compared to those in the first zone. During whisker growth, when the distance between whiskers becomes larger than the diameter of whiskers, the multilayer growth mode begins to dominate. At first, anisotropic diffusion is the major diffusion mode and mound morphology results. As the summit of the mound rises, isotropic diffusion would gradually govern the growth, and pyramidal shape appears (Fig. 4). When the pyramid is composed of enough atomic layers to realize transition from 2D ES barrier to 3D ES barrier, a new multilayered island or pyramid will nucleate and epitaxially grow on the formed ones. The summits of the pyramids of upper layer would begin to rob the diffusing clusters and adtoms, which should have contributed the growth step of the base pyramids if without ES barrier. Therefore the coarsening of the base pyramids was hindered. The more important the spherical diffusion becomes, the faster the pyramid grows. The more the top of pyramid outgrows its base, the more spherical diffusion dominates. Since the diffusion rate is faster at the summit of the pyramid, the $\{11\bar{2}3\}$ facets of the pyramid of the upper layer can completely grow themselves out of existence, leaving the slower growing $\{0001\}$ and $\{10\bar{1}0\}$ facets (Fig. 5d–f). When the summit has moved well out from the original surface and has attained a uniform cross-section, it would grow along the length at a constant rate. Then, the nanorod would grow to nanowire by repeated nucleation and growth of epitaxial hexagonal-pyramid shape-like islands (Fig. 8-4). Concurrently, the base layers of pyramid would begin to thicken themselves. The possible mechanisms of appearance of hexagonal or octagonal prisms at the bases of pyramids will be discussed later (Fig. 5d-f).

It should be emphasized that the ES barrier effect is only controlled by the crystallographic structures of the materials and temperature. The probability per unit time that an adatom diffuses to the edge of an island and descends to the lower levels instead of being reflected, divided by the rate corresponding to hopping on the terrace, varies with temperature as $\mathrm{Exp}(-\Delta\mathrm{Es}/kT)$ (ΔEs is the ES barrier height). It is reasonable to deduce that at a higher temperature, the probability is higher for adatoms to cross down the edge of the island, and ES effect can be negligible, and vice versa is true, i.e., the lower temperature, the less probability the adatom would cross down the island edge and the higher ES effect. The effect can be used to rationalize different morphology and mechanisms of ZnO nanostructures prepared at different temperatures. From the above-stated growth process combined with other studies [38, 40], it is understandable that the repeated growth of epitaxial hexagonal-pyramid shape-like islands on the positively charged (0001)-Zn plane with $\{11\bar{2}3\}$ facets as slope

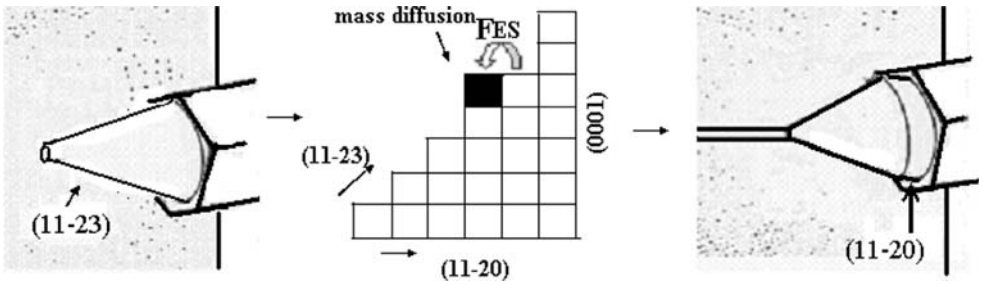

Fig. 9 Schematic of the coarsening process proposed for the base of ZnO pyramid. The black square represents the adatom. The descent of the adatom is hindered by the ES barrier at the edge of {0001} facets, which contribute to step bunching and formation of a hexagonal prism with six sidewall facets $\{11\bar{2}0\}$ (Figs. 3–5d, 3–5e) or a dodecagonal prism bounded by $\{11\bar{2}0\}$ and $\{10\bar{1}0\}$ (Figs. 3–5f)

planes are responsible for the growth of ZnO whiskers, pyramids, and nanowires in our experiments. In the preparation of ZnO nanostructures (nanowires and nanoribbons) via direct ZnO evaporation (with evaporation temperature at 1,400° and deposition temperature at 800°) [26, 27], (0001)-Zn also plays a self-catalytic role to lead the layer-by-layer growth of nanostructures without appearance of hexagonal-pyramid-shape islands because of the negligible ES effect at higher temperatures.

During coarsening of the base of pyramids, the appearance of $\{11\bar{2}0\}$ facets on the hexagonal prism or octagonal prism on the base of pyramids may be a further proof of the existence of a 2D ES barrier on (0001) facets. During coarsening, the direction of adatoms diffusing to the base of pyramid is no longer just vertical to the {0001} facets, but with a large part of vectors also parallel to {0001} facets. The adatoms therefore have more opportunity to stay on the {0001} facets and be incorporated in the step edge under the assistance of positive ES barrier on the edge of (0001) facets, which will facilitate step bunching and result in the formation of side facets $\{11\bar{2}0\}$ (Fig. 9). Actually, scanning tunneling microscopic study has revealed that $\{11\bar{2}0\}$ facets of ZnO are rough, having deep grooves with two sides parallel to the polar (0001) and $(000\bar{1})$ planes. In other words, $\{11\bar{2}0\}$ can be considered as step bunching of {0001} facets and having a similar surface cleavage energy as {0001} facets [42].

Summary

Using preparation of ZnO nanowires as an example, we elucidate the mechanisms responsible for the growth of 1D semiconducting oxide via direct evaporation of low-melting metal-Zn in O_2 atmosphere. The results indicate that the first growth stage is the nucleation of ZnO crystals on the substrate via formation of thin film. Subsequently, anisotropic abnormal growth of ZnO single crystals in the form of platelets takes place. Then, single-crystal ZnO platelets grow along the [0001] direction into the form of whiskers. During whisker growth, there exists a transformation from layer-by-layer growth to a simultaneous multilayer growth, which occurs when there is a sufficiently large 2D ES barrier at the edge of (0001) facets and the whisker diameter is smaller than the whisker spacing. The multilayer growth combined with anisotropic diffusion (linear diffusion) contributes to the formation of mounds on the upper layer of the whisker. As the top of the whiskers grows far away from the base, isotropic diffusion (spherical diffusion) replaces anisotropic diffusion (linear diffusion) resulting in the formation of pyramids. When the pyramid includes enough atomic layers to fulfill transition from 2D ES barrier to 3D ES barrier, a new multilayered pyramid or island will nucleate and grow on the old ones. When the summit of pyramid of the upper layer has moved well beyond the base surface and attained a uniform cross-section it will grow with a constant rate. The nanowires will grow in the [0001] direction by repeated nucleation and growth of epitaxial hexagonal-pyramid shape-like islands on the C-plane with $\{11\bar{2}3\}$ as the slop planes. At the same time pyramid coarsening occurs, the breakage of step motion $\{11\bar{2}3\}$ facets and the appearance of $\{11\bar{2}0\}$ facets at the corners of (0001)-Zn top planes may be further evidence for the existence of "two dimensional" ES barrier on (0001) plane of ZnO. The growth process appears to be insensitive to substrates, indicating that substrate materials have little or no influence on the growth mechanisms. Changing the reaction pressure or lowering the evaporation temperature (for example 500 °C) only reduces the diameter of the nanowires, but has no other effects on the growth process. In the formation of ZnO nanostructures, the pyramid plays a critical role as a 'bridge' to taper the whisker to nanowire with a diameter less than 100 nm. In order to form the pyramidal structure, multilayer growth and isotropic diffusion are two necessary conditions. However, the ES effect behind them is responsible for transforming microscale structure to nanoscale structure.

For the VS growth of II–VI and III–V semiconductor [8–10] nanowire, the phenomenon that nanowire grows out on large single crystal by formation of pyramid or mound

has been widely reported. The 2D and 3D ES barriers have been demonstrated to act as the bridge from micron to nano in our study. That the strength of ES barrier depends on the nature of materials and temperature has already been revealed in past research. The understanding of VS growth process of nanowire will help to take advantage of ES barrier in realizing control growth of nanowire without catalyst contamination in more material system in the future.

Acknowledgement This work is supported by the Research Grants Council of Hong Kong SAR (N_CityU125/05), China, US Army International Technology Center—Pacific, and the National Basic Research Program of China (973 Program) (Grant Nos. 2007CB936000 and 2006CB933000).

References

1. Zhong ZH, Wang DL, Cui Y, Bockrath MW, Lieber CM (2003) Science 302:1377
2. Huang Y, Duan XF, Cui Y, Lauhon LJ, Kim KH, Lieber CM (2001) Science 294:1313
3. Liu CY, Antonio J, Yao Y, Meng XM, Lee CS, Fan SS, Lifshitz Y, Lee ST (2003) Adv Mater 15:838
4. Hu J, Odom TW, Lieber CM (1999) Acc Chem Res 32:435
5. Wang ZL, Kong XY, Ding Y et al (2004) Adv Funct Mater 14:943
6. Zhang H, Zhang SY, Pan S et al (2005) J Am Ceram Soc 88:566
7. Wang N, Tang YH, Zhang YF, Lee CS, Lee ST (1998) Phys Rev B 58:R16024
8. He MQ, Zhou PZ, Mohammad SN, Harris GL, Halpern JB, Jacobs R, Sarney WL, Salamanca-Riba L (2001) J Cryst Growth 231:357
9. Wu Q, Hu Z, Wang XZ, Hu YM, Tian YJ, Chen Y (2004) Dia Rel Mat 13:38
10. Vaddiraju S, Mohite A, Chin A, Meyyappan M, Sumanasekera G, Alphenaar BW, Sunkara MK (2005) Nano Lett 5:1625
11. Sharma S, Sunkara MK (2002) J Am Chem Soc 124:12288
12. Dang HY, Wang J, Fan SS (2003) Nanotechnology 14:738
13. Lyu SC, Zhang Y, Lee CJ et al (2003) Chem Mater 15:3294
14. Zhang Y, Jia HB, Yu DP (2004) J Phys D-Appl Phys 37:413
15. Chang PC, Fan ZY, Wang D, Tseng WY, Chiou WA, Hong J, Lu JG (2004) Chem Mater 16:5133
16. Wang RC, Liu CP, Huang JL, Chen SJ (2005) Appl Phys Lett 86:251104
17. Kima TW, Kawazoe T, Yamazaki S, Ohtsu M, Sekiguchi T (2004) Appl Phys Lett 84:3358
18. Zhao M, Chen XL, Zhang XN, Dai L, Jian JK, Xu YP (2004) Appl Phys A: Mater Sci Process 79:429
19. Mozetic M, Cvelbar U, Sunkara MK, Vaddiraju S (2005) Adv Mater 17:2138
20. Brenner SS, Sears GW (1956) Acta Met 4:270
21. Zhang Y, Jia HB, Luo XH, Chen XH, Yu DP, Wang RM (2003) J Phys Chem B 107:8289
22. Kunaver U, Kolar D (1998) Acta Mater 46:4629
23. Heuer AH, Fryburg GA, Ogbuji LU, Mitchell TE, Shinozaki SJ (1978) J Am Ceram Soc 61:406
24. Mitchell TE, Ogbuji LU, Heuer AH (1978) J Am Ceram Soc 61:412
25. Meyer B, Marx D (2003) Phys Rev B 67:035403
26. Wang ZL, Kong XY, Zuo JM (2003) Phys Rev Lett 91:185502
27. Hughes WL, Wang ZL (2005) Appl Phys Lett 86:043106
28. Ehrlich G, Hudda FG (1966) J Chem Phys 44:1039
29. Schwoebel R (1969) J Appl Phys 40:614
30. Villain J (1991) J Phys I 1:19
31. Siegert M, Plischke M (1996) Phys Rev E 53:307
32. Siegert M, Plischke M (1994) Phys Rev Lett 73:1517
33. Lagally MG, Zhang ZY (2002) Nature 417:907
34. Tersoff J, Vandergon AWD, Tromp RM (1994) Phys Rev Lett 72:266
35. Kellogg GL, Feibelman PJ (1990) Phys Rev Lett 64:3143
36. Vedensky DD, Zangwill A, Luse CN, Wilby MR (1993) Phys Rev E 48:852
37. Filimonov SN, Hervieu YY (2004) Surf Sci 553:133
38. Baxter JB, Wu F, Aydila ES (2003) Appl Phys Lett 83:3797
39. Liu SJ, Huang HC, Woo CH (2002) Appl Phys Lett 80:3295
40. Isu T, Watanabe A, Hata M, Katayama Y (1988) Jpn J Appl Phys 27:L2259
41. Orme C, Johnson MD, Sudijono JL, Leung KT, Orr BG (1994) Appl Phys Lett 64:860
42. Dulub O, Boatner LA, Diebold U (2002) Surf Sci 519:201